

Syntheses, Structures, and Magnetic Properties of a Novel *mer*-[(bbp)Fe^{III}(CN)₃]²⁻ Building Block (bbp: bis(2-benzimidazolyl)pyridine dianion) and Its Related Heterobimetallic Fe(III)–Ni(II) Complexes

Anangamohan Panja,^{*,†,‡} Philippe Guionneau,^{†,‡} Je-Rang Jeon,^{†,‡,§,||} Stephen M. Holmes,^{⊥,⊗} Rodolphe Clérac,^{§,||} and Corine Mathonière^{*,†,‡}

[†]CNRS, ICMCB, UPR 9048, F-33600 Pessac, France

[‡]Univ. of Bordeaux, ICMCB, UPR 9048, F-33600 Pessac, France

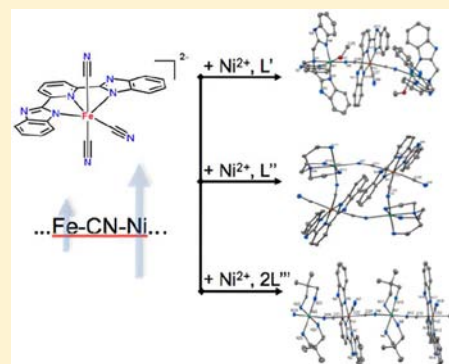
[§]CNRS, CRPP, UPR 8641, F-33600 Pessac, France

^{||}Univ. of Bordeaux, CRPP, UPR 8641, F-33600 Pessac, France

[⊥]Department of Chemistry and Biochemistry and [⊗]Center for Nanoscience, University of Missouri—St. Louis, Missouri 63121, United States

S Supporting Information

ABSTRACT: A new symmetrical tricyanide building block *mer*-[Fe(bbpcy)₃]²⁻ [1; bbpcy = bis(2-benzimidazolyl)pyridine dianion] has been prepared and structurally and magnetically characterized. It forms a new low-spin meridionally capped {Fe^{III}L(CN)₃} fragment with the tridentate bbpcy ligand. The reaction of 1 with Ni^{II} salts in the presence of various ancillary ligands affords several new cyanido-bridged complexes: a trinuclear complex {[Ni(ntb)(MeOH)]₂[Fe(bbpcy)(CN)₃][ClO₄]₂}·2MeOH (2), a tetranuclear compound {[Ni(tren)]₂[Fe(bbpcy)(CN)₃]₂}·7MeOH (3), and a one-dimensional heterobimetallic system: {[Ni(dpd)]₂[Fe(bbpcy)(CN)₃]₂}·9MeOH·3H₂O (4) [ntb = tris(2-benzimidazolylmethyl)amine, tren = tris(2-aminoethyl)amine, and dpd = 2,2-dimethyl-1,3-propanediamine]. The structural data shows that 2 is a linear complex in which a central Fe^{III} ion links two adjacent Ni^{II} ions via axial cyanides, while 3 is a molecular square that contains cyanido-bridged Ni^{II} and Fe^{III} ions at alternate corners. Complex 4 is a one-dimensional system that is composed of alternating cyanido-bridged Ni^{II} and Fe^{III} centers. Compounds 2–4 display extensive hydrogen bonding and moderately strong π – π stacking interactions in the solid state. Magnetic studies show that ferromagnetic exchange is operative within the Fe^{III}_{LS}(μ -CN)Ni^{II} units of 2–4.



INTRODUCTION

Over the past two decades, there has been intense research in cyanide-based materials owing to the diverse ranges of topologically unique structures, optical, and magnetic properties.¹ Among these, those that exhibit high temperature magnetic order,² photoresponsive properties,³ spin-crossover (SCO),⁴ chirality,⁵ single-molecule magnet⁶ (SMM) and single-chain magnet⁷ (SCM) behaviors are of particular interest for applications. The most common examples contain hexacyanidometalates, [M(CN)₆]³⁻ (M = Fe^{III}, Cr^{III}, Mn^{III}, etc.), which in the presence of reactive metal complexes form robust M-(μ -CN)-M' linkages. In the absence of capping ligands (e.g., hydrated Mⁿ⁺ ions) three-dimensional lattices known collectively as Prussian blue analogues are the most commonly encountered structural archetype.^{3a,b,8} Unfortunately single crystal studies of these insoluble materials are generally difficult to obtain and are limited to a few examples. To isolate new types of structures based on the same hexacyanidometalate building blocks, a typically employed strategy utilizes multi-dentate ligands to limit the numbers of M-(μ -CN)-M' units

formed during the assembly reactions. Judicious choice of ancillary ligands and building blocks allow for the engineering of discrete and well-defined complexes (including high-spin species and SMMs) in addition to a diverse assortment of 1-D, 2-D, and 3-D cyanidometalate materials. Of the latter, several systems exhibit long-range magnetic order above room temperature, photoresponsive behavior, and slow relaxation of the magnetization (SCMs).^{3c,d,6,7,9}

In this research field, the use of versatile building blocks of general formula [FeL(CN)_x]⁻ (L = a polydentate ligand; x = 2–4) have led to numerous new cyanido-bridged low-dimensional heterometallic systems with interesting properties.¹⁰ The introduction of well-designed blocking ligands for the cyanide precursors plays a crucial role as it can control the nuclearity, topology, and the dimensionality of resulting products. Among this large family, several tricyanidoferrate(III) complexes utilize tridentate and facially coordinate blocking

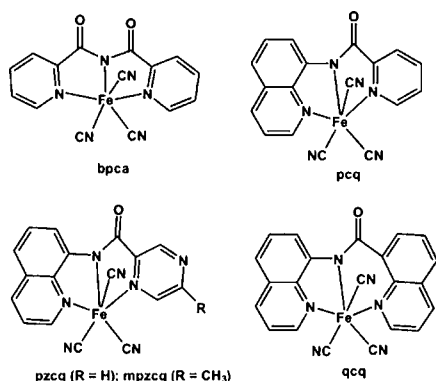
Received: July 30, 2012

Published: November 7, 2012

groups: hydrotris(pyrazol-1-yl)borate (Tp), hydrotris(3,5-dimethylpyrazol-1-yl)borate (Tp*), tetra(pyrazol-1-yl)borate (pzTp), and 1,3,5-triaminocyclohexane (tach).^{11–15} These tricyanidoferrate(III) precursors have led to a large number of cyanido-bridged bimetallic complexes containing $\text{Fe}^{\text{III}}(\mu\text{-CN})\text{M}^{\text{II}}$ units. Among these, $\{\text{Fe}_2\text{Ni}_2\}$ squares,¹³ and $\{\text{Fe}_4\text{Ni}_4\}$ ¹⁴ cubic complexes and several one-dimensional systems containing $\text{Fe}^{\text{III}}(\mu\text{-CN})\text{Ni}^{\text{II}}$ units,¹⁶ exhibit very interesting magnetic properties such as SMM, SCM, and magneto-chiral behavior. Recently, we and others have found that similar objects containing $\text{Fe}^{\text{III}}(\mu\text{-CN})\text{Co}^{\text{II}}$ units based on $\{\text{Fe}_2\text{Co}_2\}$ and $\{\text{Fe}_4\text{Co}_4\}$ cores show evidence of tunable magnetic and optical properties because of a thermal-induced and photoinduced electron transfer.¹⁷

Along with facially capped $[\text{Fe}(\text{L})(\text{CN})_3]^-$ compounds, some meridionally capped precursors have been described in the literature using chelating ligands containing a variety of bis(2-pyridylcarbonyl)amidate anion (bpca) or their derivatives [Scheme 1]:^{18–22} 8-(pyridine-2-carboxamido)quinoline (pcq),

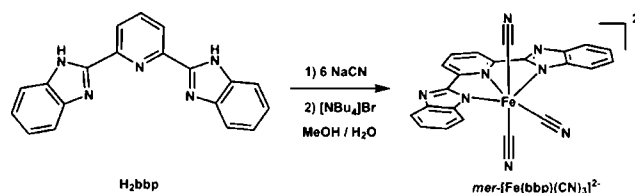
Scheme 1. Schematic Representations of $mer\text{-}[(\text{L})\text{Fe}^{\text{III}}(\text{CN})_3]^-$ Tricyanide Building Blocks and the Different Capping Ligands



8-(pyrazine-2-carboxamido)quinoline (pzcq), 8-(5-methylpyrazine-2-carboxamido)quinoline (mpzqc), and 8-(2-quinoline-2-carboxamido)quinoline anion (qcq). Surprisingly, few studies have investigated the assembly reactions and materials properties of those constructed from these $mer\text{-}[(\text{L})\text{Fe}^{\text{III}}(\text{CN})_3]^-$ anions. When amide or imide functionalities are present, the majority of known cyanidometalate complexes containing these ligands are coordinated to di- and trivalent manganese centers.^{18–22}

Thus, we initiated the use of meridionally tricyanide building blocks to construct polynuclear complexes and chains that could potentially exhibit interesting magnetic properties.²³ Under the assumption that the charge will play a key role in the assembly process, we limited our initial investigations to tricyanide complexes containing the bis(2-benzimidazolyl)pyridine dianion (bbp^{2-}). This bbp ligand has a planar geometry that enforces meridional coordination geometry. The further excess addition of cyanide in solution containing Fe^{3+} and bbp^{2-} would likely afford a $mer\text{-}[(\text{bbp})\text{Fe}^{\text{III}}(\text{CN})_3]^{2-}$ complex [Scheme 2]. Herein we report on the syntheses, structures, and magnetic properties of this new dianionic tricyanide complex, and on several cyanido-bridged polynuclear complexes formed with this building block.

Scheme 2. Synthesis of $mer\text{-}[(\text{bbp})\text{Fe}^{\text{III}}(\text{CN})_3]^{2-}$ 1



EXPERIMENTAL SECTION

Materials and Physical Measurements. All chemicals and solvents were reagent grade and were used as received. Bis(2-benzimidazolyl)pyridine (H_2bbp) and tris(2-benzimidazolylmethyl)amine (ntb) were prepared according to literature methods.²⁴ Elemental analyses for C, H, and N were conducted using the Pregl-Dumas technique on a Thermo Fischer Flash EA1112 analyzer. FT-IR spectra were recorded in the 400–4000 cm^{-1} range on a Nicolet 750 Magna-IR spectrometer using KBr pellets. Magnetic measurements performed on polycrystalline samples (20.32, 15.38, 10.01, and 10.64 mg for **1**, **2**, **3**, and **4**, respectively) placed in small polyethylene bags ($3 \times 0.5 \times 0.02$ cm) were carried out on a Quantum Design MPMS-XL SQUID magnetometer. Experimental data were corrected for sample holder and diamagnetic contribution of the samples.

Caution! Perchlorate salts are potentially explosive, and cyanides are very toxic. Thus, these materials should be handled in small quantities and with great care. Waste solutions containing cyanide were oxidized via basic sodium hypochlorite to afford the corresponding aqueous cyanate solution.

Synthesis of $[\text{NBu}_4]_2[\text{Fe}(\text{bbp})(\text{CN})_3] \cdot 3\text{H}_2\text{O}$ (1**).** Addition of H_2bbp (3.13 g, 10.0 mmol) diluted in methanol (20 mL) to a methanol solution (60 mL) of $\text{FeCl}_3 \cdot 6\text{H}_2\text{O}$ (2.70 g, 10.0 mmol) afforded a red solution that was refluxed for 1 h. An aqueous solution (40 mL) of NaCN (2.94 g, 60.0 mmol) was then added to the reaction. After an additional 8 h reflux, the solution became dark blue, and the mixture was subsequently filtered. The filtrate was concentrated via rotary evaporation to about 30 mL volume. Solid $[\text{NBu}_4]\text{Br}$ (3.22 g, 10.0 mmol) was added to the filtrate, and a blue crystalline solid precipitated. The blue microcrystals were isolated via suction filtration, washed with water (2×10 mL), and dried under vacuum at room temperature for 12 h. Dark blue crystals suitable for single crystal X-ray analysis were obtained via slow evaporation of a methanol solution containing **1** at room temperature within one week. Yield: 8.74 g (89%). Anal. Calcd. for $\text{C}_{54}\text{H}_{89}\text{FeN}_{10}\text{O}_3$: C, 66.03; H, 9.13; N, 14.26. Found: C, 66.10; H, 9.24; N, 14.11. IR (KBr, cm^{-1}): 3442 (br; $\bar{\nu}_{\text{NH, OH}}$); 2961 (s), 2935 (m), 2873 (s; $\bar{\nu}_{\text{C-H}}$); 1615 (m; $\bar{\nu}_{\text{C=N}}$), 2113 (sh, s; $\bar{\nu}_{\text{CN}}$) and 2105 (s; $\bar{\nu}_{\text{CN}}$).

Synthesis of $[\text{Ni}(\text{ntb})(\text{MeOH})_2][\text{Fe}(\text{bbp})(\text{CN})_3] \cdot [\text{ClO}_4]_2 \cdot 2\text{MeOH}$ (2**).** A stoichiometric mixture of $\text{Ni}(\text{ClO}_4)_2 \cdot 6\text{H}_2\text{O}$ (73.1 mg, 0.20 mmol) and ntb (81.4 mg, 0.20 mmol) was dissolved in methanol (20 mL) to afford a pale pink solution that was subsequently added with stirring to **1** (98.2 mg, 0.10 mmol, 1:2 Fe:Ni stoichiometry) diluted in methanol (20 mL). The green solution was allowed to slowly evaporate, and X-ray quality green crystals were obtained after 1 week. The remaining crystals of **2** were isolated via suction filtration, washed with methanol (2×5 mL), and dried in air. Yield: 0.102 g (58%). Anal. Calcd. for $\text{C}_{76}\text{H}_{75}\text{Cl}_2\text{FeN}_{22}\text{Ni}_2\text{O}_{14}$: C, 51.73; H, 4.28; N, 17.46. Found: C, 51.58; H, 4.32; N, 17.31. IR (KBr, cm^{-1}): 3361 (s, br; $\bar{\nu}_{\text{NH, OH}}$); 1615 (m; $\bar{\nu}_{\text{C=N}}$), 2152 (m; $\bar{\nu}_{\text{CN}}$), 2106 (w; $\bar{\nu}_{\text{CN}}$).

Synthesis of $[\text{Ni}(\text{tren})_2][\text{Fe}(\text{bbp})(\text{CN})_3]_2 \cdot 7\text{MeOH}$ (3**).** Solid $\text{Ni}(\text{NO}_3)_2 \cdot 6\text{H}_2\text{O}$ (58.2 mg, 0.20 mmol) and tren (29.2 mg, 0.20 mmol) were dissolved in methanol (20 mL) to afford a green solution. Addition of a methanolic solution (20 mL) of **1** (196 mg, 0.20 mmol, 1:1 Fe:Ni stoichiometry) afforded a blue-green solution that was stirred for 10 min at room temperature. Slow evaporation over 2 days afforded copious quantities of green block crystals that were suitable for single crystal X-ray analysis. The remaining crystals were isolated via suction filtration, washed with methanol (2×5 mL), and air-dried at room temperature. Yield: 0.096 g (64%). Anal. Calcd. for $\text{C}_{63}\text{H}_{82}\text{Fe}_2\text{N}_{24}\text{Ni}_2\text{O}_7$: C, 49.89; H, 5.45; N, 22.16. Found: C, 49.78;

Table 1. Selected Crystal Data and Structure Refinement Parameters of 1–4

	1	2	3	4
formula	C ₅₄ H ₉₅ FeN ₁₀ O ₆	C ₇₆ H ₇₇ Cl ₂ FeN ₂₂ Ni ₂ O ₁₄	C ₆₃ H ₈₂ Fe ₂ N ₂₄ Ni ₂ O ₇	C ₁₄₇ H ₂₃₆ Fe ₄ N ₄₈ Ni ₄ O ₂₂
M/g mol ⁻¹	1036.25	1766.76	1516.65	3486.08
T/K	100(2)	150(2)	150(2)	150(2)
λ/Å	0.71073	0.71073	0.71073	0.71073
crystal system	monoclinic	monoclinic	monoclinic	monoclinic
space group	P2 ₁	C2/c	P2 ₁ /c	P2 ₁ /c
a/Å	21.267(2)	35.374(9)	11.560(2)	19.175(3)
b/Å	11.4830(13)	10.983(3)	23.814(6)	19.260(4)
c/Å	26.049(3)	26.094(6)	13.475(3)	26.279(5)
β (deg)	111.875(2)	128.75(1)	105.20(1)	91.893(1)
V/Å ³	5903.4(11)	7905.9(3)	3580.04(14)	9700.5(3)
Z	4	4	2	2
d _{calc} /g cm ⁻³	1.166	1.483	1.407	1.193
abs. coeff. (mm ⁻¹)	0.309	0.799	0.983	0.737
F(000)	2252	3652	1584	3692
crystal size/mm	0.2 × 0.10 × 0.02	0.25 × 0.12 × 0.08	0.30 × 0.10 × 0.05	0.40 × 0.32 × 0.06
θ range/deg	2.35–25.38	2.0–27.51	3.15–27.51	1.50–27.48
limiting indices	–25 ≤ h ≤ 18, –13 ≤ k ≤ 13, –30 ≤ l ≤ 31	–45 ≤ h ≤ 45, –13 ≤ k ≤ 14, –33 ≤ l ≤ 33	–14 ≤ h ≤ 15, –30 ≤ k ≤ 30, –17 ≤ l ≤ 17	–24 ≤ h ≤ 24, –24 ≤ k ≤ 24, –34 ≤ l ≤ 34
refl. collected/unique	39068/20672	15958/8969	16129/8180	42504/22114
indep. reflect./R _{int}	12994/0.0375	6387/0.0299	5733/0.0409	12229/0.717
completeness to 2θ (%)	0.95	0.987	0.994	0.995
data/restraints/parameters	20672/660/1337	8969/6/548	8180/0/499	22114/18/1050
goodness-of-fit on F ^{2c}	1.028	1.038	1.036	1.040
R ₁ ^a , wR ₂ ^b [I > 2σ(I)]	0.084, 0.212	0.055, 0.152	0.043, 0.106	0.073, 0.199
R ₁ ^a , wR ₂ ^b	0.1395, 0.2525	0.086, 0.177	0.077, 0.120	0.146, 0.236
largest diff. peak, hole in e Å ⁻³	0.85/–0.41	1.03/–0.65	0.88/–0.65	1.72/–0.91
Flack parameter	–0.001			

^aR₁ = $\sum ||F_o| - |F_c|| / \sum |F_o|$. ^bwR₂ = $[\sum [w(F_o^2 - F_c^2)^2] / \sum [w(F_o^2)^2]]^{1/2}$; $w = 1/[\sigma^2(F_o^2) + (aP)^2 + bP]$ where $P = [\max(F_o^2 \text{ or } 0) + 2(F_o^2)]/3$. ^cGoodness of fit: GOF = $[\sum w(F_o^2 - F_c^2)^2 / (n - p)]^{1/2}$, where n is the number of reflections and p is the number of parameters.

H, 5.32; N, 22.29. IR (KBr, cm⁻¹): 3424 (br; $\bar{\nu}_{\text{NH, OH}}$); 1610 (m; $\bar{\nu}_{\text{C=N}}$); 2116 (m; $\bar{\nu}_{\text{CN}}$); 2148 (w; $\bar{\nu}_{\text{CN}}$).

Synthesis of {[Ni(dpd)₂][Fe(bbp)(CN)₃]}·9MeOH·3H₂O (4). Addition of 2,2-dimethyl-1,3-propanediamine (dpd) (20.4 mg, 0.20 mmol) diluted in methanol (10 mL) to a methanol (10 mL) solution of Ni(NO₃)₂·6H₂O (29.1 mg, 0.10 mmol) afforded a blue-green solution. A methanol solution (20 mL) of solution of **1** (98.2 mg, 0.10 mmol, 1:1 Fe:Ni stoichiometry) was then added to the reaction. The solution was stirred for 10 min at room temperature, and the mixture was left to concentrate in air. X-ray quality crystals were obtained after 4 days. The remaining crystals were isolated via suction filtration, washed with methanol (2 × 5 mL), and air-dried at room temperature. Yield: 0.046 g (53%). Anal. Calcd. for C₇₃H₁₀₅Fe₂N₂₄Ni₂O₁₂: C, 50.52; H, 6.14; N, 19.24. Found: C, 50.38; H, 6.32; N, 19.09. IR (KBr, cm⁻¹): 3406 (s, br; $\bar{\nu}_{\text{NH, OH}}$), 1611 (m; $\bar{\nu}_{\text{C=N}}$), 2108 (m; $\bar{\nu}_{\text{CN}}$), 2132 (w; $\bar{\nu}_{\text{CN}}$).

Structural Studies. Single crystal X-ray diffraction data for **1–4** were collected on a Nonius Kappa CCD diffractometer using monochromatized Mo- α radiation ($\lambda = 0.71073$ Å). Crystals were mounted on glass fibers using N-Paratone oil and cooled in situ using an Oxford Cryostream 600 Series using the stream of nitrogen gas (150 K). Several scans in φ and ω directions were made to increase the number of redundant reflections and were averaged during refinement cycles. Intensities were integrated using DENZO-SMN and scaled with SCALEPACK.²⁵ The structures were solved by direct methods, and all non-hydrogen atoms were refined using anisotropic thermal parameters via a full-matrix least-squares-based method on F² using the SHELXL-97²⁶ program within the WINGX package.²⁷ Hydrogen atoms bound to carbon were placed in calculated positions using a riding model while those attached to some methanol lattice solvents were located in the difference Fourier map and refined using fixed isotropic thermal parameters based on their respective parent

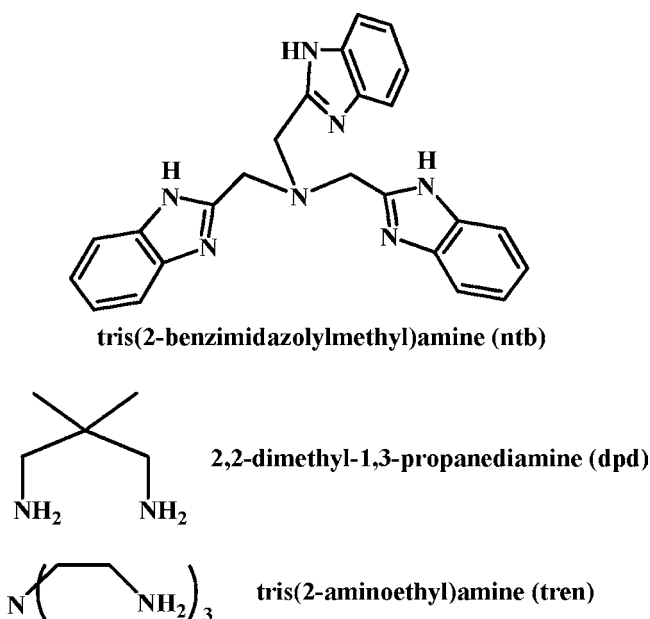
atoms. The crystallographic data for compounds **1–4** are found in Table 1. Crystallographic data (excluding structure factors) for the structure reported in this paper have been deposited at the Cambridge Data Centre as supplementary publication nos. CCDC-891990 for **1**, CCDC-891991 for **2**, CCDC-891992 for **3**, CCDC-891993 for **4**. Copies of the data can be obtained free of charge on application to CCDC, 12 Union Road, Cambridge CB21EZ, UK (fax: (+44) 1223–336–033; email: deposit@ccdc.cam.ac.uk).

RESULTS AND DISCUSSION

Synthesis and Characterization. Treatment of H₂bbp with FeCl₃·6H₂O in the presence of an excess of NaCN readily affords *mer*-[Fe(bbp)(CN)₃]²⁻ in high yield (≈ 90%). Fortuitously, the presence of the metal ion in excess aqueous cyanide is sufficiently basic to deprotonate the H₂bbp ligand in situ [Scheme 2]. The corresponding tetrabutylammonium derivative (**1**) is easily prepared via addition of [NBu₄]Br to the crude reaction mixture. Complex **1** is soluble in most common polar organic solvents (e.g., MeCN, MeOH, CH₂Cl₂, and DMF) making it a promising building unit for the construction of multinuclear complexes and chain derivatives.

Addition of **1** to methanolic solutions of nickel(II) salts and three different multidentate ligands L' [Scheme 3] in different ratios affords three polynuclear complexes which contain the *mer*-[Fe(bbp)(CN)₃]²⁻ building unit and cyanido bridges between Fe^{III} and Ni^{II} ions. In the presence of **1**, solutions containing Ni(ClO₄)₂·6H₂O and ntb in a 1:1 ratio afford {[Ni(ntb)(MeOH)]₂[Fe(bbp)(CN)₃]}·[ClO₄]₂·2MeOH (**2**) as a dicationic trinuclear {Ni^{II}₂Fe^{III}} complex, suggesting that

Scheme 3. Ancillary Ligands Present in $[\text{Ni}^{\text{II}}(\text{L})_n]^{2+}$ Fragments of 2–4



reactive $[\text{cis-Ni}^{\text{II}}(\text{ntb})(\text{solv})_2]^{2+}$ complexes are formed in solution. In comparison, addition of **1** to 1:1 or 1:2 methanolic mixtures of $\text{Ni}(\text{NO}_3)_2 \cdot 6\text{H}_2\text{O}$ and more flexible tren or dpd ligands afford $\{[\text{Ni}(\text{tren})]_2[\text{Fe}(\text{bbp})(\text{CN})_3]_2\} \cdot 7\text{MeOH}$ (**3**) as a neutral tetranuclear $\{\text{Ni}^{\text{II}}_2\text{Fe}^{\text{III}}_2\}$ complex while $\{[\text{Ni}(\text{dpd})]_2[\text{Fe}(\text{bbp})(\text{CN})_3]_2\} \cdot 9\text{MeOH} \cdot 3\text{H}_2\text{O}$ (**4**) is a one-dimensional neutral $\{\text{Ni}^{\text{II}}\text{Fe}^{\text{III}}\}$ system. Moreover, investigations with different Fe:Ni stoichiometries, as 1:1 or 1:2 or 2:1 ratio of the two reactants, exclusively resulted in the same three compounds, suggesting that the reaction stoichiometry is not crucial for the formation of the three complexes. Consequently, the overall connectivity and the nuclearity of the final complexes seem to be governed by (i) the neutralization charge of the formed species as shown for **3** and **4** and (ii) the number and the geometrical arrangement of labile coordination sites of the intermediate $[\text{Ni}^{\text{II}}(\text{L})(\text{solv})_n]^{2+}$ complexes formed in situ for the isolation of the three compounds.

The infrared spectra of **1–4** display cyanide stretching absorptions that are characteristic of those seen for low spin tricyanidoferrate(III) complexes.^{11–19} For example the high-energy $\bar{\nu}_{\text{CN}}$ absorptions $[2113, 2106 \text{ cm}^{-1}]$ seen in **1** indicate that the iron center is trivalent as reported for a variety of tricyanometalates. As it is typical for polynuclear complexes containing $[(\text{L})\text{Fe}^{\text{III}}_{\text{LS}}(\text{CN})_3]^{n-}$ units, the infrared spectra for **2–4** suggest that both bridging and terminal cyanides are present.^{11–19} For **2** and **3**, the infrared spectra exhibit two $\bar{\nu}_{\text{CN}}$ stretches $[2152 \text{ and } 2106 \text{ cm}^{-1}]$ for **2**; $2152 \text{ and } 2116 \text{ cm}^{-1}$ for **3** with one being shifted to higher energy relative to those seen for **1**, suggesting that $\{\text{Fe}^{\text{III}}(\mu\text{-CN})\text{Ni}^{\text{II}}\}$ motifs are present. Additional intense perchlorate $\bar{\nu}_{\text{Cl-O}}$ stretches $[1109 \text{ and } 625 \text{ cm}^{-1}]$ are also found in the infrared spectrum of **2** suggesting that it contains a cationic cyanido bridged species. Mirroring the above trends compound **4** displays two cyanido stretching absorptions at $2122 \text{ and } 2108 \text{ cm}^{-1}$, respectively.^{11–19,28} We tentatively ascribe the lower energy absorptions present in the infrared spectra of **2–4** as belonging to terminal cyanides.

Structural Studies. The sheet-like blue crystals of **1** have been obtained by slow evaporation of the methanol/water

solution. The compound crystallizes in the monoclinic $P2_1$ space group and consists of $[\text{Fe}(\text{bbp})(\text{CN})_3]^{2-}$ anions, tetrabutylammonium cations, and crystallization solvent molecules that are water and methanol. For the anion, the tridentate N_3 planar ligand (bbp) coordinates the iron(III) center in a meridional fashion and the three cyanide ligands occupy the remaining meridional sites (Figure 1 and Supporting

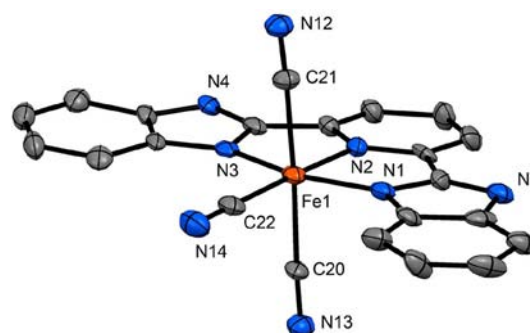


Figure 1. Ortep type view of the molecular structure of **1**. Thermal ellipsoids are at the 30% level and all lattice solvents, tetrabutylammonium ions, and hydrogen atoms are omitted for clarity.

Information, Figure S1). The distances between the iron(III) and the nitrogen of the bbp ligand vary in the range of $1.936(6)–1.974(5) \text{ \AA}$ (Table 2), considerably shorter than the reported distances for high spin iron(III) complexes with the similar ligand, $\{\text{Fe}(\text{Me}_2\text{-bbp})\text{Cl}_3\}$ ($2.111(3)–2.168(3) \text{ \AA}$).²⁸ These bond distances together with the Fe–C distances ($1.903(8)–1.978(7) \text{ \AA}$) are in good agreement with those reported for the other cyanido-containing mononuclear iron(III) low-spin complexes. The iron(III) ion has distorted octahedral coordination geometry mainly because of the geometrical requirement of the bbp ligand. The uncoordinated nitrogen on the imidazole rings of the ligand and the nitrogen from the cyanides are interacting with the crystallization water molecules through the hydrogen bonds to form an extensive network. The void spaces in **1** are occupied by Bu_4N^+ cations that are extremely disordered.

Compound **2** crystallizes as a trinuclear complex in the monoclinic $C2/c$ space group (Figure 2 and Table 1). The cationic trinuclear $\{\text{Ni}^{\text{II}}_2\text{Fe}^{\text{III}}\}$ complex is composed of two $[\text{Ni}^{\text{II}}(\text{ntb})]^{2+}$ cations linked via cyanides to a central $\text{mer}[(\text{bbp})\text{Fe}^{\text{III}}(\text{CN})_3]^{2-}$ forming a $\text{trans}\{-\text{Fe}(\mu\text{-CN})_2\text{Ni}_2\}$ unit; a terminal cyanide remains and is perpendicular to the long axis of **2**. Complex **2** is a quite unusual complex considering that the majority of $[(\text{L})\text{Fe}^{\text{III}}(\text{CN})_3]^{2-}$ or 4^- complexes typically form neutral trinuclear $\{\text{Fe}^{\text{III}}_2\text{Ni}^{\text{II}}\}$ complexes (*cis* and *trans*) where a central Ni^{II} center is linked to two adjacent Fe^{III} ions via cyanide bridges.^{7a,12} In structure of **2**, the iron center adopts a meridional arrangement of cyanides as a consequence of the tridentate bbp^{2-} ligand (Figure 2). The Fe–C [$1.902(5)$ and $1.946(3) \text{ \AA}$] and Fe–N [$1.938(4)$ to $1.946(3) \text{ \AA}$] distances are comparable to those seen in a variety of cyanoferrate(III) complexes and the iron site adopts a distorted $\text{mer}[\text{FeN}_3\text{C}_3]$ coordination geometry (Table 2).^{11–19,28} The remaining *cis*- $[\text{Ni}^{\text{II}}(\text{ntb})(\mu\text{-NC})(\text{MeOH})]^{2+}$ fragments are related by 2-fold symmetry. The Ni–N bonds range between $1.998(3) \text{ \AA}$ [Ni1–N8] for the bridging cyanide, and $2.040(3) \text{ \AA}$ and $2.211(3) \text{ \AA}$ [Ni1–N6 and Ni1–N1], for those belonging to the ntb ligand.³⁰ The terminal Fe–CN angles are linear while those of the bridging cyanides [within the $\text{Fe}(\mu\text{-CN})\text{Ni}$ units] are close

Table 2. Selected Bond Distances (Å) and Angles (deg) in 1–4

	1	2	3	4			
Fe1–N1	1.934(6)	Ni1–O1	2.195(3)	Ni1–N7	2.065(2)	Ni1–N6	2.093(4)
Fe1–N2	1.953(6)	Ni1–N2	2.064(3)	Ni1–N10	2.124(2)	Ni1–N9	2.129(4)
Fe1–N3	1.938(6)	Ni1–N6	2.040(3)	Ni1–N12	2.108(2)	Ni1–N11	2.120(4)
Fe1–C20	1.961(7)	Ni1–N1	2.211(3)	Ni1–N9	2.107(2)	Ni2–N19	2.108(4)
Fe1–C21	1.974(7)	Ni1–N4	2.053(3)	Ni1–N11	2.101(2)	Ni2–N21	2.119(4)
Fe1–C22	1.952(9)	Ni1–N8	1.998(3)	Ni1–N8	2.113(2)	Ni2–N23	2.107(5)
Fe2–N6	1.947(5)	Fe1–N10	1.946(3)	Fe1–N1	1.936(2)	Fe1–N1	1.943(4)
Fe2–N7	1.960(5)	Fe1–C26	1.946(3)	Fe1–N5	1.937(2)	Fe1–N5	1.936(4)
Fe2–N8	1.945(6)	Fe1–N12	1.938(4)	Fe1–C21	1.966(3)	Fe1–C21	1.941(5)
Fe2–C42	1.964(7)	Fe1–C27	1.902(5)	Fe1–N3	1.934(2)	Fe2–N17	1.928(4)
Fe2–C43	1.971(7)			Fe1–C20	1.963(3)	Fe2–C53	1.932(5)
Fe2–C44	1.903(8)	Ni1–N8–C26	176.5(3)	Fe1–C22	1.919(3)	Ni1–N8	2.108(5)
		Fe1–C27–N9	180.0(1)			Ni1–N10	2.116(4)
N3–Fe1–N1	161.0(3)	Fe1–C26–N8	174.2(3)	Ni1–N8–C22	164.3(2)	Ni1–N12	2.039(4)
N3–Fe1–N2	80.1(2)	Fe1–C27–N9	180.0(1)	Ni1–N7–C21	149.4(2)	Ni2–N20	2.134(5)
N1–Fe1–N2	81.0(2)			Fe1–C20–N6	176.9(2)	Ni2–N22	2.118(4)
N2–Fe1–C22	178.5(3)			Fe1–C22–N8	173.7(2)	Ni2–N24	2.050(4)
N13–C20–Fe1	177.4(7)			Fe1–C21–N7	172.1(2)	Fe1–N3	1.939(4)
N12–C21–Fe1	178.1(7)					Fe1–C20	1.940(5)
N14–C22–Fe1	179.4(8)					Fe1–C22	1.910(5)
N16–C43–Fe2	179.4(8)					Fe2–C33	1.941(5)
C44–Fe2–N6	178.0(3)					Fe2–C54	1.962(5)
N8–Fe2–N6	81.2(2)						
N8–Fe2–N7	162.1(2)					Fe1–C20–N6	171.6(4)
N6–Fe2–N7	81.0(2)					Fe1–C22–N7	178.7(5)
N15–C44–Fe2	177.4(8)					Fe2–C53–N18	179.4(5)
N17–C42–Fe2	178.7(6)					Ni1–N6–C20	148.9(4)
						Ni2–N19–C54	148.6(4)
						Fe1–C21–N24	176.3(5)
						Fe2–C33–N12	176.6(5)
						Fe2–C54–N19	170.3(4)
						Ni1–N12–C33	167.3(4)
						Ni2–N24–C21	166.0(4)

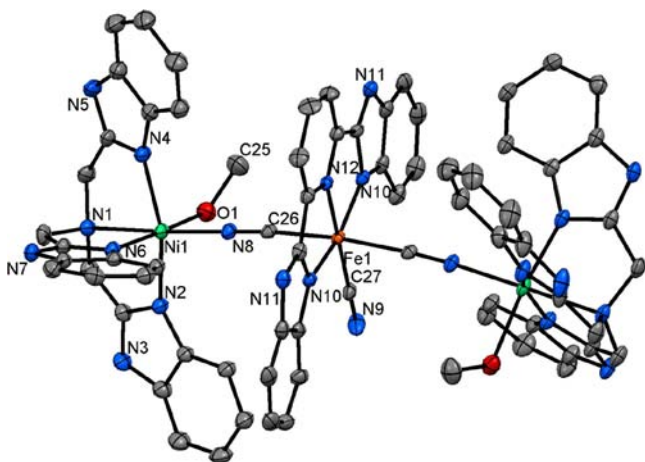


Figure 2. Ortep type view of the crystal structure of **2**. Thermal ellipsoids are at the 30% level and all lattice solvents, ClO_4^- anions, and hydrogen atoms are omitted for clarity.

to linearity, being $174.2(3)^\circ$ and $176.5(3)^\circ$, for Fe1–C26–N8 and Ni1–N8–C26, respectively. The intramolecular Fe \cdots Ni and Ni \cdots Ni distances are 5.08 and 10.05 Å, respectively, while the intermolecular Ni \cdots Ni, Fe \cdots Ni, and Fe \cdots Fe ones are 8.96, 10.63, and 10.98 Å, respectively. Additionally intermolecular π – π interactions [ca. 3.58 Å] are found between the adjacent

bbp aromatic rings and are found to propagate along the crystallographic *b* direction (Supporting Information, Figure S2).

Compound **3** crystallizes as a centrosymmetric tetranuclear complex in the monoclinic $P2_1/c$ space group (Table 1, Figure 3). The structure of **3** consists of *mer*-[Fe^{III}(bbp)(CN)₃]²⁻ and [Ni^{II}(tren)]²⁺ centers that occupy alternate corners of the neutral {Fe^{III}₂Ni^{II}₂} square complex; complex **3** is unique in that the majority of the known {Fe^{III}₂M^{II}₂} molecular squares are dications while **3** has a neutral charge overall.^{16,28b,31} As seen in structures of **1** and **2**, the Fe centers adopt distorted octahedral geometries. The Fe–N_{bbp} distances range from 1.934(2) [Fe1–N3] to 1.937(2) Å [Fe1–N5], while the Fe–C ones vary from 1.919(3) [Fe1–C22] to 1.966(3) Å [Fe1–C21], being similar to those seen in the structures of **1** and **2** (Table 2).^{7a,32} In **3**, the Fe–C–N angles range between $172.1(2)^\circ$ [Fe1–C21–N7] and $176.9(2)^\circ$ [Fe1–C20–N6] suggesting that the {Fe₂Ni₂} core suffers from greater steric congestion than that within **2**. The Ni^{II} ions are highly distorted, owing the increased steric demand of the tren ligand.^{14,16,31} The Ni–N_{tren} bonds vary slightly between 2.101(2) and 2.124(2) Å [for Ni1–N11 and Ni1–N10], while those belonging to the bridging cyanides range from 2.065(2) to 2.113(2) Å, for Ni1–N7 and Ni1–N8, respectively (Table 2). Likewise, the Ni–NC angles are significantly distorted in comparison to those seen in structure of **2**, ranging

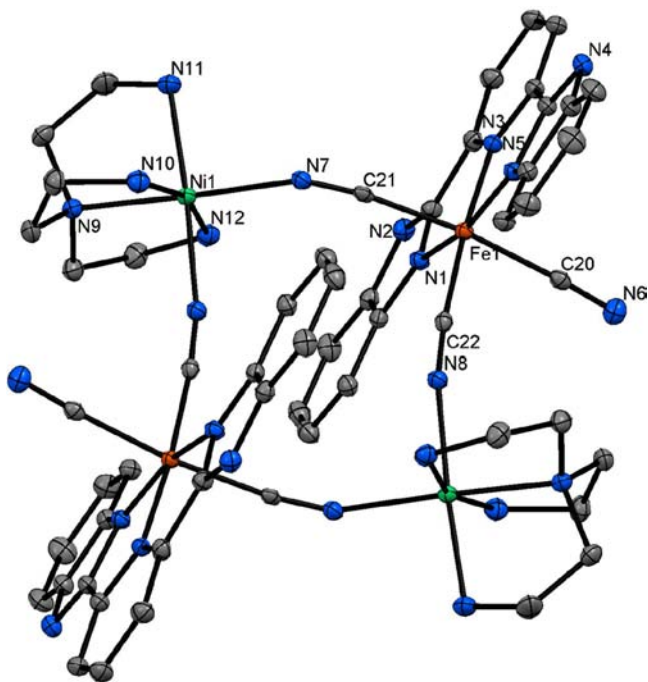


Figure 3. Ortep view of the crystal structure of **3**. Thermal ellipsoids are at the 30% level and all lattice solvent and hydrogen atoms are omitted for clarity.

from $149.4(2)^\circ$ [Ni1–N7–C21] to $164.3(2)^\circ$ [Ni1–N8–C22], being comparable to those seen in a variety of cationic $\{\text{Fe}^{\text{III}}\text{Ni}^{\text{II}}\}_2$ complexes.^{31,33}

Within the $\{\text{Fe}_2\text{Ni}_2\}$ core, the Fe···Ni distances are 4.94 Å and 5.11 Å, while the diagonal Ni···Ni and Fe···Fe distances are 7.16 and 7.05 Å, respectively; the closest intermolecular metal–metal contacts are 7.84 Å [Fe···Ni]. As in the structure of **2**, extensive π – π interactions between adjacent pyridyl groups of bbp ligand afford a supramolecular arrangement along the crystallographic *c* direction (Supporting Information, Figure S3). These close contacts [ca. 3.28 Å] are also accompanied by extensive hydrogen bonding interactions within the *bc* plane between lattice methanol, nitrogen, atoms belonging to terminal cyanides, tren and bbp ligands.

Compound **4** crystallizes as a chain within the monoclinic $P2_1/c$ space group (Table 1). The chains consist of an alternating array of crystallographically independent two sets of *trans*-[Ni(dpd)₂(μ -NC)₂] and *mer*-[Fe(bbp)(μ -CN)₂(CN)] fragments connected via bridging cyanides along the crystallographic *a* direction (Figure 4 and Supporting Information, Figure S4). The average Ni–N_{dpd} [ca. 2.12(1) Å], Ni–N_{CN} [ca. 2.07(1) Å], and Fe–C [ca. 1.93(1) Å] bonds are within the typical ranges.^{16,31,34} In comparison, the Fe–N bonds display a greater range of values [1.924(4) to 1.943(4) Å] and are comparable to those seen in **1**, **2**, and **3** (Table 2).

The Fe–C–N bond angles are nearly linear for terminal cyanides while bridging ones are significantly distorted. For example, the Fe1–C22–N7 and Fe2–C53–N18 angles [$178.7(5)^\circ$ and $179.4(5)^\circ$] suggest little steric interactions are present between ancillary ligands, while those engaged in the formation of Fe–CN–Ni units are highly distorted, and range from $170.3(4)^\circ$ to $176.6(5)^\circ$, for Fe2–C54–N19 and Fe2–C33–N12, respectively; the Ni–N≡C angles are also nonlinear and range between $148.9(4)^\circ$ [Ni1–N6–C20] and $167.3(4)^\circ$ [Ni1–N12–C33]. As before, π – π stacking and hydrogen

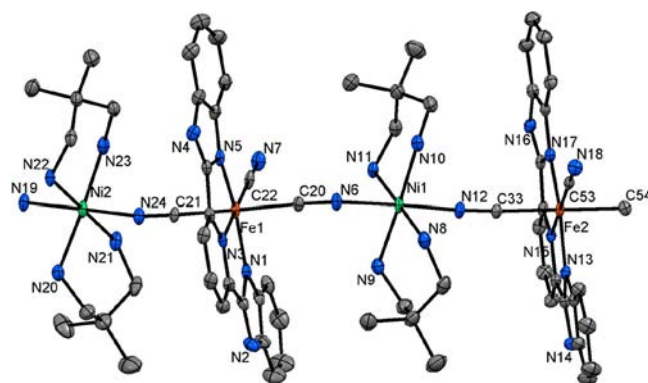


Figure 4. Ortep view of the asymmetric unit in **4**. Thermal ellipsoids are at the 30% level and all lattice solvent and hydrogen atoms are eliminated for clarity.

bonding interactions between adjacent bbp and cyanide ligands and lattice methanol are also observed and stabilize additional interchain interactions perpendicular to the crystallographic *a* direction (Supporting Information, Figure S4). Lastly, slightly shorter intrachain Fe···Ni [e.g., 4.92 Å, Fe1···Ni1] and interchain metal–metal distances of 8.51 Å (Ni1···Ni2) and 9.65 Å (Ni1···Fe1) are found in **4**.

Magnetic Properties. The magnetic properties of **1–4** were studied as the thermal dependence between 1.8 and 290 K for the χT products (where χ is the molar magnetic susceptibility defined by M/H , M being the magnetization and H the external magnetic field fixed at 1 kOe) and as the field dependence of M below 8 K. The temperature dependence of χT product for **1** shows that it remains nearly constant [ca. $0.47 \text{ cm}^3 \text{ K mol}^{-1}$] in the 1.8–280 K range as expected for isolated magnetic species and thus a paramagnetic Curie behavior (Supporting Information, Figure S5). This value is higher than the expected value [$0.375 \text{ cm}^3 \text{ K mol}^{-1}$] for a complex which contains isolated and isotropic $S = 1/2$ ions, suggesting that orbital contributions to the magnetic moment are present and leading to a *g* value of about 2.2(1).^{11,16} Consistent with this assumption fitting of the M vs H curve measured at 1.8 K with an $S = 1/2$ Brillouin function indicates that *g* is equal to 2.29(1), a value that is consistent with those reported for other low spin cyanidoferrate(III) complexes.^{11,19}

The static magnetic properties of **2** were also investigated over a temperature range of 1.8 to 290 K, and are shown in Figure 5 as the thermal dependence of the χT product (per $\{\text{Fe}^{\text{III}}\text{Ni}^{\text{II}}\}_2$ unit). At room temperature, the χT product ($3.02 \text{ cm}^3 \text{ K mol}^{-1}$) is slightly higher than that expected [$2.9 \text{ cm}^3 \text{ K mol}^{-1}$] for a non-interacting $\text{Fe}^{\text{III}}_{\text{LS}}$ ($S = 1/2$ with $g = 2.29$ as determined for **1**) and Ni^{II} ($S = 1$ with $g = 2.2$) ions in a 1:2 ratio. As the temperature is lowered, the χT product gradually increases until 8 K, where a maximum value of $4.68 \text{ cm}^3 \text{ mol}^{-1}$ K is attained. At lower temperatures, the χT value decreases toward a minimum of $3.38 \text{ cm}^3 \text{ K mol}^{-1}$ at 1.8 K. The lack of a minimum in the χT vs T curve between 8 and 290 K is suggestive of dominating ferromagnetic interactions between the Fe^{III} and the Ni^{II} ions in **2**. Moreover, additional evidence for ferromagnetic exchange interactions being dominant within **2** is found in the field saturation of the magnetization data. A value of $\sim 5.30 \mu_{\text{B}}$ under an applied 70 kOe magnetic field at 1.8 K confirms that **2** adopts an $S_{\text{T}} = 5/2$ ground state (Supporting Information, Figure S6).

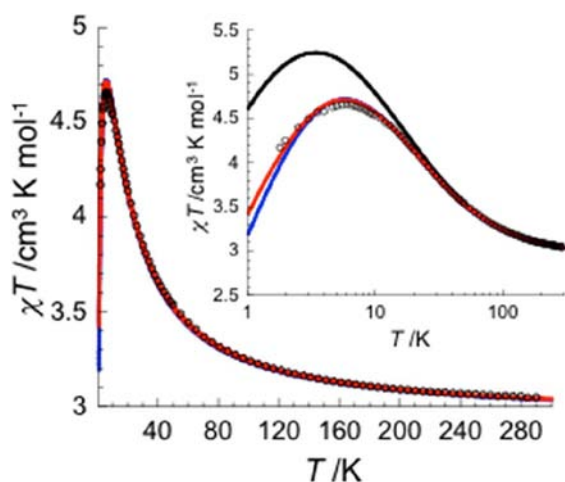


Figure 5. Temperature dependence of the χT product for **2** (where $\chi = M/H$ per complex) measured at $H = 0.1$ T. Inset: Expansion view of the main figure in semilogarithmic plot. The solid lines are the best fits to the models described in the text.

Using the structure of **2** as a guide, the molar magnetic susceptibility $\chi_{\text{Ni}_2\text{Fe}}$ was first derived using an isotropic Heisenberg Hamiltonian, $\hat{H} = -2J S_{\text{Fe}} \cdot (S_{\text{Ni}_1} + S_{\text{Ni}_2})$, in which equivalent exchange constants (J) between the central Fe^{III} and the two external Ni^{II} ions were considered (eq 1).³⁵ Additional $\text{Ni} \cdots \text{Ni}$ interactions were not considered as part of the model given that about 10 Å separates the Ni^{II} ions. However to fit properly the data intercomplex interactions (through the zJ' exchange constants) were considered in the frame of the mean-field approximation (eq 2):

$$\chi_{\text{Ni}_2\text{Fe}} T = \frac{N\mu_{\text{B}}^2}{4k_{\text{B}}} g^2 \times \frac{10 + e^{J/k_{\text{B}}T} + e^{3J/k_{\text{B}}T} + 10e^{4J/k_{\text{B}}T} + 35e^{5J/k_{\text{B}}T}}{2 + e^{J/k_{\text{B}}T} + e^{3J/k_{\text{B}}T} + 2e^{4J/k_{\text{B}}T} + 3e^{5J/k_{\text{B}}T}} \quad (1)$$

$$\chi = \frac{\chi_{\text{Ni}_2\text{Fe}}}{1 - \frac{2zJ'}{N\mu_{\text{B}}^2 g^2} \chi_{\text{Ni}_2\text{Fe}}} \quad (2)$$

Indeed fitting the χT vs T data collected for **2** via eqs 1 and 2 in the 1.8–290 K temperature range affords the red line in Figure 5 with $g = 2.22(1)$, $J/k_{\text{B}} = +12.4(2)$ K, and $zJ'/k_{\text{B}} = -0.09(1)$ K. The positive value of exchange coupling J through the cyanido bridges confirms that ferromagnetic interactions are operative between the Ni^{II} and Fe^{III} centers. Thus the spin ground state of **2** is $S_{\text{T}} = 5/2$. We note that the magnitude of the exchange coupling (J) within **2** is comparable to those seen when linear $\text{Fe}^{\text{III}}(\mu\text{-CN})\text{Ni}^{\text{II}}$ linkages are present.^{12a,13c,36b} The negative value of zJ' suggests that weak antiferromagnetic interactions between $\{\text{Ni}_2\text{Fe}\}$ complexes are present. Nevertheless it is worth mentioning that these interactions are certainly overestimated by this first magnetic model as their estimation also contains phenomenologically the effects of the magnetic anisotropy brought by the $\text{Ni}(\text{II})$ ions. Therefore an alternative model has been used to estimate the magnetic anisotropy parameter, D_{Ni} . Considering the following Hamiltonian $\hat{H} = -2J S_{\text{Fe}} \cdot (S_{\text{Ni}_1} + S_{\text{Ni}_2}) + D_{\text{Ni}} (S_{z,\text{Ni}_1}^2 + S_{z,\text{Ni}_2}^2)$, the M vs H data between 1.8 and 8 K have been numerically calculated using the MAGPACK program,³⁷ and compared with the experimental data. The best simulation shown in red

lines in Supporting Information, Figure S6 corresponds to $g_{\text{Ni}} = 2.21(1)$, $g_{\text{Fe}} = 2.29(1)$, $J/k_{\text{B}} = +12.4(2)$ K, and $D_{\text{Ni}}/k_{\text{B}} = -4(1)$ K. This D_{Ni} value is in the range of ones found in similar Ni complexes.^{38,39} Then these parameters have been used in the MAGPACK program to reproduce the χT vs T curve (black line) and compared with the experimental values (inset in Figure 5). This simulation is quite good down to 25 K, but below this temperature a large deviation with the experimental data is observed caused by the presence of weak intercomplex interactions that have negligible effect on M vs H curves, but are observed in the χT vs T curve. Therefore, taking into account these intercomplex interactions using eq 2 with the simulated MAGPACK χT values for $\chi T_{\text{Ni}_2\text{Fe}}$, we obtained the blue curve with $zJ'/k_{\text{B}} = -0.05(1)$ K (inset in Figure 5). However, even if this second modelization approach seems more physically reasonable, it does not improve the quality of the fits. Therefore, the obtained values for the $D_{\text{Ni}}/k_{\text{B}}$ and zJ'/k_{B} parameters must be taken with caution as they produce similar effects on magnetic properties and they can not be estimated independently with a good accuracy.

For **3**, the χT vs T data (where χ is the molar magnetic susceptibility per $\{\text{Fe}^{\text{III}}_2\text{Ni}^{\text{II}}_2\}$ unit) over the temperature range of 1.8–290 K is shown in Figure 6. At 290 K, the χT product

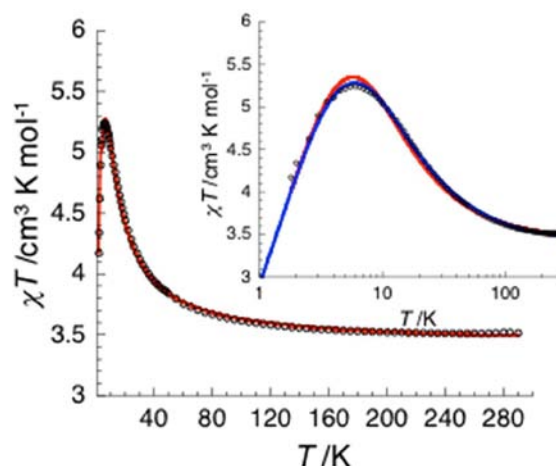


Figure 6. Temperature dependence of the χT product of **3** (where $\chi = M/H$ per complex) measured at $H = 0.1$ T. Inset: Expansion view of the main figure in semilogarithmic plot. The solid lines are the best fits to the models described in the text.

($3.52 \text{ cm}^3 \text{ mol}^{-1} \text{ K}$) is slightly higher to the anticipated values [$3.40 \text{ cm}^3 \text{ K mol}^{-1}$] for a 2:2 ratio of uncoupled $\text{Fe}^{\text{III}}_{\text{LS}}$ and Ni^{II} ions considering $g_{\text{Fe}} = 2.29$ and $g_{\text{Ni}} = 2.2$. Upon cooling, the χT value gradually increases toward a maximum of $5.24 \text{ cm}^3 \text{ K mol}^{-1}$ at 8 K, suggesting that ferromagnetic interactions are also operative in **3**. Decreasing the temperature further affords smaller χT values, and a value of $4.18 \text{ cm}^3 \text{ K mol}^{-1}$ is found at 1.8 K. The field dependence of the magnetization at 1.8 K also confirms that the paramagnetic ions are engaged in ferromagnetic interactions. The saturation magnetization at 7 T is about $6.34 \mu_{\text{B}}$ and is indicative of an $S_{\text{T}} = 3$ magnetic ground state for **3** (Supporting Information, Figure S7).

Using the rectangular structure of **3** as a guide, the magnetic data can be analyzed using a derived equation obtained from the isotropic Heisenberg Hamiltonian $\hat{H} = -2J_1 (S_{\text{Fe}_1} \cdot S_{\text{Ni}_1} + S_{\text{Fe}_2} \cdot S_{\text{Ni}_2}) - 2J_2 (S_{\text{Fe}_1} \cdot S_{\text{Ni}_2} + S_{\text{Fe}_2} \cdot S_{\text{Ni}_1})$, where two exchange interactions between adjacent Ni^{II} and Fe^{III} ions are

considered.³⁴ An analytical expression of the χT is only available when $J_1 = J_2 = J$ and is given by eq 3:

$$\chi_{\text{Ni}_2\text{Fe}_2} T = \frac{2N\mu_{\text{B}}^2}{k_{\text{B}}} g^2 \times \frac{1 + 6e^{4J/k_{\text{B}}T} + 5e^{8J/k_{\text{B}}T} + 7e^{6J/k_{\text{B}}T} + 14e^{10J/k_{\text{B}}T}}{3 + e^{2J/k_{\text{B}}T} + 8e^{4J/k_{\text{B}}T} + 12e^{6J/k_{\text{B}}T} + 5e^{8J/k_{\text{B}}T} + 7e^{10J/k_{\text{B}}T}} \quad (3)$$

We have first used this expression to fit the magnetic data for **3**, considering a modified expression of eq 2 to take into account the intercomplex interactions (where $\chi_{\text{Ni}_2\text{Fe}_2}$ is replaced by $\chi_{\text{Ni}_2\text{Fe}_2}$). The best set of parameters to reproduce the experimental data are $g = 2.23(1)$; $J/k_{\text{B}} = +4.41(2)$ K, $z'/k_{\text{B}} = -0.11(1)$ K (red line in Figure 6). The J parameter is positive confirming the ferromagnetic interactions between the Fe(III) and Ni(II) ions through the cyanido bridges. Then, we have also simulated these data using the two- J (J_1 and J_2) model using the MAGPACK program and found the best simulation with the following parameters $g_{\text{Ni}} = 2.21(1)$; $g_{\text{Fe}} = 2.29(1)$, $J_1/k_{\text{B}} = +7.0(2)$ K, $J_2/k_{\text{B}} = +3.0(2)$ K, $z'/k_{\text{B}} = -0.19(1)$ K (blue line inset of Figure 6). The two interactions parameters are both positive and are in the range of the values obtained for other ferromagnetically coupled $\text{Fe}^{\text{III}}(\mu\text{-CN})\text{Ni}^{\text{II}}$ squares.^{13c} In both models, the intercomplex interactions given by z' have been found to be equal but they are likely overestimated as they contain phenomenologically the intercomplex interactions and the magnetic single-ion anisotropy brought by the Ni(II) ions. Similarly to the magnetic analysis made for **2**, we have tried to extract the Ni(II) anisotropy from the simulation with MAGPACK of the M vs H curves. But no reasonable physical solutions were found probably due to the effect of the intercomplex interactions that are much larger in **3** than in **2**.

For **4**, the χT vs T data normalized by FeNi units are shown in Figure 7. At 290 K, the χT product ($1.95 \text{ cm}^3 \text{ K mol}^{-1}$) is

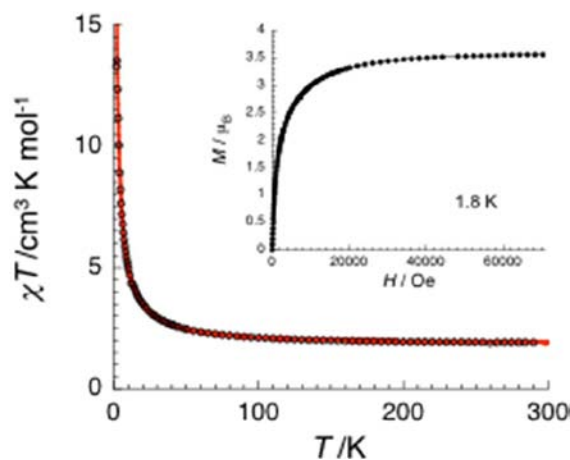


Figure 7. Temperature dependence of the χT product for **4** (where $\chi = M/H$ per FeNi units) measured at $H = 0.1$ T. Inset: Field dependence of the magnetization at 1.8 K for **4**. The solid red lines are the best fit to a Seiden model described in the text.

higher than the expected value ($1.70 \text{ cm}^3 \text{ K mol}^{-1}$) for a 1:1 ratio of magnetically independent $\text{Fe}^{\text{III}}_{\text{LS}}$ and Ni^{II} ions considering $g_{\text{Fe}} = 2.29$ and $g_{\text{Ni}} = 2.2$. As it is typical for ferromagnetically coupled compounds, the χT values gradually increase with decreasing the temperature and reach a maximum of $13.5 \text{ cm}^3 \text{ K mol}^{-1}$ at 2 K, before slightly decreasing to 13.3

$\text{cm}^3 \text{ K mol}^{-1}$ at 1.8 K. The M vs H data also supports the assumption that the exchange interactions in **4** are ferromagnetic (Figure 7), as a magnetization value of $\sim 3.6 \mu_{\text{B}}$ is reached at 70 kOe and 1.8 K.

On the basis of the chain structure, the theoretical temperature dependence of the χT product can be expressed in the frame of the Seiden model derived from the isotropic exchange spin Hamiltonian $H = -2J \sum_i (S_{\text{Ni},i} + S_{\text{Ni},i+1}) \cdot S_{\text{Fe},i}$ where the S_{Ni} is considered as a classical spin ($S_{\text{Ni}} = 1$) and S_{Fe} as a quantum spin ($S_{\text{Fe}} = 1/2$).⁴⁰ It is worth mentioning that the Seiden model has been already used for another reported alternating $S = 1 - s = 1/2$ chain and the obtained magnetic coupling J was supported by theoretical density functional theory (DFT) calculations.⁴¹ Using this model for **4**, the χT vs T data in the 2–290 K range was fitted as shown in Figure 7. The best set of parameters are $g = 2.30(1)$ and $J/k_{\text{B}} = +18.5(2)$ K, confirming that **4** is a ferromagnetically coupled chain. To check if this J/k_{B} value is correctly estimated by the Seiden model, we used this J value of $18.5(2)$ K in the MAGPACK program³⁷ to simulate the magnetic data of chains formed by rings of up to 12 magnetic centers (or 6 $S = 1 - s = 1/2$ units) where the two spins are treated as quantum spins. The experimental χT vs T data are also correctly reproduced with this model down to 10 K validating the J value found with the Seiden model. Below 10 K, the simulated χT data are much smaller than the experimental ones, this difference being obviously attributed to the limited number of spins within the rings considered in the MAGPACK calculations.

Considering the hypothesis that compounds **2–4** contain symmetrical octahedral metal ions, strict orthogonality of the π symmetry $\text{Fe}^{\text{III}}_{\text{LS}} (t_{2g}^5 e_g^0)$ and σ symmetry $\text{Ni}^{\text{II}} (t_{2g}^6 e_g^2)$ orbitals leads to a ferromagnetic coupling arrangement by satisfying Hund's rule. The magnitude of the exchange couplings found for **2–4** are in the typical range [$1.7\text{--}24.6$ K] observed for complexes containing $\text{Fe}^{\text{III}}_{\text{LS}}(\mu\text{-CN})\text{Ni}^{\text{II}}$ linkages.^{12–14,16,28b,30d,31,36,38} On the basis of numerous examples of $\text{Fe}^{\text{III}}\text{--Ni}^{\text{II}}$ cyanido-bridged compounds with similar architectures (Supporting Information, Table S1), we have tried to identify magneto-structural correlations in these systems. Unfortunately no evident relation between the magnetic exchange coupling and a single structural parameter was found, suggesting that several structural factors may indeed be relevant such as Ni-NC angles, but also Ni...Fe metal separations and/or torsion angles. However, in our series of compounds obtained with the same Fe(III) precursor, we observe that the magnitude of the Fe(III)–Ni(II) exchange coupling is strongly dependent on the cyanido geometry around the Fe center. Large ferromagnetic interactions are found when the coordinated cyanido groups are in trans positions, as shown by the high values of $J/k_{\text{B}} = +12.4$ K and $J/k_{\text{B}} = +18.5$ K estimated for **2** and **4**, respectively. In comparison, a smaller J/k_{B} value ($= +4.4$ K) is found for the distorted square in **3** where the coordinating cyanido groups are in cis positions. This result is in agreement with an optimized orthogonality of the magnetic orbitals with the trans-bridging geometry. These conclusions should be taken with caution, and also corroborated with other compounds that can be obtained with **1** in a near future.

Unfortunately, none of our bimetallic systems present slow relaxation of their magnetization. The lack of slow dynamics was initially surprising given that structurally related tetranuclear $\{\text{fac-Fe}^{\text{III}}_2\text{Ni}^{\text{II}}_2\}$ complexes are reported to be SMMs.¹³ Nevertheless, it is likely that the magnetic anisotropy

brought by **1** is not sufficient ($g = 2.29$) compared to those found in the related *fac*-(L)Fe(CN)₃ complexes, where $g \sim 2.9$. Reduction in orbital symmetry in **1**, from C_{3v} [for *fac*-Fe(CN)₃] units toward idealized C_{2v}, likely acts to quench the orbital contributions to the magnetic moment.

CONCLUSIONS

In summary, a new *mer*-tricyanidoiron(III) building block, **1**, involving a dianionic form of the benzimidazolyl ligand has been successfully synthesized. Using this dianionic precursor, we have synthesized and structurally characterized a trinuclear {Fe^{III}Ni^{II}} complex (**2**), a tetranuclear rectangular {Fe^{III}₂Ni^{II}₂} complex (**3**), and a bimetallic 1D system (**4**). The investigation of their magnetic properties undoubtedly reveals an overall ferromagnetic interaction between Fe(III) and Ni(II) centers via the cyanido group. The magnitude of the Fe(III)–Ni(II) magnetic coupling is clearly related to the linearity of the Ni(II)–NC–Fe(III)–CN–Ni(II) motif. Although, slow relaxation of the magnetization was not detected above 1.8 K, we think that our synthetic strategy for designing and synthesizing a new versatile building block will have a big impact for the preparation of novel cyanido-bridged molecular materials having interesting magnetic properties. Future work utilizing this building unit will involve the synthesis of zero or low-dimensional Mn(III)–Fe(III) and Co(II)–Fe(III) complexes that may exhibit SCM or SMM behavior and photoinduced properties, respectively.

ASSOCIATED CONTENT

Supporting Information

Further details are given in Figures S1–S7 and Table S1. This material is available free of charge via the Internet at <http://pubs.acs.org>.

AUTHOR INFORMATION

Corresponding Author

*E-mail: ampanja@yahoo.co.in (A.P.), mathon@icmcb-bordeaux.cnrs.fr (C.M.).

Notes

The authors declare no competing financial interest.

ACKNOWLEDGMENTS

A.P. gratefully acknowledges the Erasmus Mundus Mobility in Asia and External Cooperation Window (EMMA-ECW) for postdoctoral fellowship support. C.M. acknowledges the Institut Universitaire de France (IUF) for financial support. R.C. and C.M. acknowledge the University of Bordeaux, ANR (NT09_469563, AC-MAGnets project), Région Aquitaine, GIS Advanced Materials in Aquitaine (COMET Project), and the CNRS for financial support. S.M.H. thanks the National Science Foundation (CAREER, CHE 0914935) and Missouri Research Board for financial support. The authors would like to thank Pierre Dechambenoit for his help on the X-ray structure resolution of the compound **1**.

REFERENCES

(1) (a) Dunbar, K. R.; Heintz, R. A. *Prog. Inorg. Chem.* **1997**, *45*, 283. (b) Verdager, M.; Bleuzen, A.; Marvaud, V.; Vaissermann, J.; Desplanches, C.; Sculler, A.; Train, C.; Garde, R.; Gelly, G.; Lomenech, C.; Rosenman, I.; Veillet, P.; Cartier dit Moulin, C.; Villain, F. *Coord. Chem. Rev.* **1999**, *190–192*, 1023. (c) Shatruck, M.; Avendaño, C.; Dunbar, K. R. *Prog. Inorg. Chem.* **2009**, *56*, 155.

(2) (a) Entley, W. R.; Girolami, G. S. *Science* **1995**, *268*, 397. (b) Ferlay, S.; Mallah, T.; Ouahès, R.; Veillet, P.; Verdager, M. *Nature* **1995**, *378*, 701. (c) Sato, O.; Iyoda, T.; Fujishima, A.; Hashimoto, K. *Science* **1996**, *271*, 49. (d) Hatlevik, Ø.; Buschmann, W. E.; Zhang, J.; Manson, J. L.; Miller, J. S. *Adv. Mater.* **1999**, *11*, 914. (e) Holmes, S. M.; Girolami, G. S. *J. Am. Chem. Soc.* **1999**, *121*, 5593. (f) Lü, Z.; Wang, X.; Liu, Z.; Liao, F.; Gao, S.; Xiong, R.; Ma, H.; Zhang, D.; Zhu, D. *Inorg. Chem.* **2006**, *45*, 999.

(3) (a) Sato, O.; Iyoda, T.; Fujishima, A.; Hashimoto, K. *Science* **1996**, *272*, 704. (b) Bleuzen, A.; Lomenech, C.; Escax, V.; Villain, F.; Varret, F.; Cartier dit Moulin, C.; Verdager, M. *J. Am. Chem. Soc.* **2000**, *122*, 6648. (c) Herrera, J. M.; Marvaud, V.; Verdager, M.; Marrot, J.; Kalisz, M.; Mathonière, C. *Angew. Chem., Int. Ed.* **2004**, *43*, 5468. (d) Long, J.; Chamoreau, L.-M.; Mathonière, C.; Marvaud, V. *Inorg. Chem.* **2008**, *47*, 22. (e) Bleuzen, A.; Marvaud, V.; Mathonière, C.; Sieklucka, B.; Verdager, M. *Inorg. Chem.* **2009**, *48*, 3453. (f) Verdager, M.; Girolami, G. S. In *Magnetism-Molecules to Materials*; Miller, J. S., Drillon, M., Eds.; Wiley-VCH: Mannheim, Germany, 2005; Vol. 5.

(4) (a) Niel, V.; Thompson, A. L.; Muñoz, M. C.; Galet, A.; Goeta, A. E.; Real, J. A. *Angew. Chem., Int. Ed.* **2003**, *42*, 3760. (b) Nihei, M.; Ui, M.; Yokota, M.; Han, L.; Maeda, A.; Kishida, H.; Okamoto, H.; Oshio, H. *Angew. Chem., Int. Ed.* **2005**, *44*, 6484. (c) Cobo, S.; Molnar, G.; Real, J. A.; Bousseksou, A. *Angew. Chem., Int. Ed.* **2006**, *45*, 5786. (d) Shatruck, M.; Dragulescu-Andrasi, A.; Chambers, K. E.; Stoian, S. A.; Bominaar, E. L.; Achim, C.; Dunbar, K. R. *J. Am. Chem. Soc.* **2007**, *129*, 6104. (e) Volatron, F.; Catala, L.; Rivière, E.; Gloter, A.; Stephan, O.; Mallah, T. *Inorg. Chem.* **2008**, *47*, 6584. (f) Martínez, V.; Boldog, I.; Gaspar, A. B.; Ksenofontov, V.; Bhattacharjee, A.; Gülich, P.; Real, J. A. *Chem. Mater.* **2010**, *22*, 4271.

(5) (a) Coronado, E.; Gómez-García, C. J.; Nuez, A.; Romero, F. M.; Waerenborgh, J. C. *Chem. Mater.* **2006**, *18*, 2670. (b) Kaneko, W.; Kitagawa, S.; Ohba, M. *J. Am. Chem. Soc.* **2007**, *129*, 248. (c) Sereda, O.; Ribas, J.; Stoeckli-Evans, H. *Inorg. Chem.* **2008**, *47*, 5107. (d) Wang, C. F.; Li, D. P.; Chen, X.; Li, X. M.; Li, Y. Z.; Zuo, J. L.; You, X. Z. *Chem. Commun.* **2009**, 6940. (e) Shiga, T.; Newton, G. N.; Mathieson, J. S.; Tetsuka, T.; Nihei, M.; Cronin, L.; Oshio, H. *Dalton Trans.* **2010**, 39, 4730.

(6) (a) Sokol, J. J.; Hee, A. G.; Long, J. R. *J. Am. Chem. Soc.* **2002**, *124*, 7656. (b) Berlinguette, C. P.; Vaughn, D.; Cañada-Vilalta, C.; Galán-Mascarós, J. R.; Dunbar, K. R. *Angew. Chem., Int. Ed.* **2003**, *42*, 1523. (c) Schelter, E. J.; Prosvirin, A. V.; Reiff, W. M.; Dunbar, K. R. *Angew. Chem., Int. Ed.* **2004**, *43*, 4912. (d) Schelter, E. J.; Prosvirin, A. V.; Dunbar, K. R. *J. Am. Chem. Soc.* **2004**, *126*, 15004. (e) Wang, C.-F.; Zuo, J.-L.; Bartlett, B. M.; Song, Y.; Long, J. R.; You, X.-Z. *J. Am. Chem. Soc.* **2006**, *128*, 7162. (f) Freedman, D. E.; Jenkins, D. M.; Iavarone, A. T.; Long, J. R. *J. Am. Chem. Soc.* **2008**, *130*, 2884. (g) Sutter, J.-P.; Dhers, S.; Rajamani, R.; Ramasesha, S.; Costes, J.-P.; Duhayon, C.; Vendier, L. *Inorg. Chem.* **2009**, *48*, 5820. (h) Goodwin, A. L.; Kennedy, B. J.; Kepert, C. J. *J. Am. Chem. Soc.* **2009**, *131*, 6334.

(7) (a) Choi, H. J.; Sokol, J. J.; Long, J. R. *Inorg. Chem.* **2004**, *43*, 1606. (b) Ferbinteau, M.; Miyasaka, H.; Wernsdorfer, W.; Nakata, K.; Sugiura, K.; Yamashita, M.; Coulon, C.; Clérac, R. *J. Am. Chem. Soc.* **2005**, *127*, 3090. (c) Toma, L. M.; Lescouëzec, R.; Pasan, J.; Ruiz-Perez, C.; Vaissermann, J.; Cano, J.; Carrasco, R.; Wernsdorfer, W.; Lloret, F.; Julve, M. *J. Am. Chem. Soc.* **2006**, *128*, 4842. (d) Choi, S. W.; Kwak, H. Y.; Yoon, J. H.; Kim, H. C.; Koh, E. K.; Hong, C. S. *Inorg. Chem.* **2008**, *47*, 10214. (e) Miyasaka, H.; Julve, M.; Yamashita, M.; Clérac, R. *Inorg. Chem.* **2009**, *48*, 3420. (f) Harris, T. D.; Bennett, M. V.; Clérac, R.; Long, J. R. *J. Am. Chem. Soc.* **2010**, *132*, 3980.

(8) (a) Buschmann, W. E.; Miller, J. S. *Inorg. Chem.* **2000**, *39*, 2411. (b) Margadonna, S.; Prassides, K.; Fitch, A. N. *Angew. Chem., Int. Ed.* **2004**, *43*, 6316. (c) Coronado, E.; Gimenez-Lopez, M. C.; Levchenko, G.; Romero, F. M.; Garcia-Baonza, V.; Milner, A.; Paz-Pasternak, M. *J. Am. Chem. Soc.* **2005**, *127*, 4580. (d) Escax, V.; Champion, G.; Arrio, M.-A.; Zacchigna, M.; Cartier dit Moulin, C.; Bleuzen, A. *Angew. Chem., Int. Ed.* **2005**, *44*, 4798. (e) Kaye, S. S.; Long, J. R. *J. Am. Chem. Soc.* **2005**, *127*, 6506. (f) Tokoro, H.; Matsuda, T.; Nuida, T.; Moritomo, Y.; Ohoyama, K.; Davy, Loutete Dnagui, E.;

- Boukheddaden, K.; Ohkoshi, S.-i. *Chem. Mater.* **2008**, *20*, 423.
- (g) Maurin, I.; Chernyshov, D.; Varret, F.; Bleuzen, A.; Tokoro, H.; Hashimoto, K.; Ohkoshi, S.-i. *Phys. Rev. B.* **2009**, *79*, 64420.
- (h) Ohkoshi, S.-i.; Nakagawa, K.; Tomono, K.; Imoto, K.; Tsunobuchi, Y.; Tokoro, H. *J. Am. Chem. Soc.* **2010**, *132*, 6620.
- (9) (a) Van Langenberg, K.; Batten, S. R.; Berry, K. J.; Hockless, D. C. R.; Moubarak, B.; Murray, K. S. *Inorg. Chem.* **1997**, *36*, 5006. (b) Marvaud, V.; Decroix, C.; Scullier, A.; Tuyères, F.; Guyard-Duhayon, C.; Vaissermann, J.; Marrot, J.; Gonnet, F.; Verdaguer, M. *Chem.—Eur. J.* **2003**, *9*, 1692. (c) Berlinguette, C. P.; Dragulescu-Andrasi, A.; Sieber, A.; Güdel, H. U.; Achim, C.; Dunbar, K. R. *J. Am. Chem. Soc.* **2005**, *127*, 6766. (d) Zhang, Y.-J.; Liu, T.; Kanegawa, S.; Sato, O. *J. Am. Chem. Soc.* **2009**, *131*, 7942. (e) Funck, K. E.; Hilfiger, M. G.; Berlinguette, C. P.; Shatrak, M.; Wernsdorfer, W.; Dunbar, K. R. *Inorg. Chem.* **2009**, *48*, 3438. (f) Maxim, C.; Sorace, L.; Khuntia, P.; Madalan, A. M.; Kravtsov, V.; Lascialfari, A.; Caneschi, A.; Journaux, Y.; Andruh, M. *Dalton Trans.* **2010**, *39*, 4838.
- (10) (a) Wen, H.-R.; Wang, C.-F.; Song, Y.; Gao, S.; Zuo, J.-L.; You, X.-Z. *Inorg. Chem.* **2006**, *45*, 8942. (b) Gu, Z.-G.; Yang, Q.-F.; Liu, W.; Song, Y.; Li, T.-Z.; Zuo, J.-L.; You, X.-Z. *Inorg. Chem.* **2006**, *45*, 8895. (c) Wang, S.; Zuo, J.-L.; Zhou, H.-C.; Choi, H. J.; Ke, Y.; Long, J. R.; You, X.-Z. *Angew. Chem., Int. Ed.* **2004**, *43*, 5940. (d) Wang, S.; Ding, X.-H.; Zuo, J.-L.; You, X.-Z.; Huang, W. *Coord. Chem. Rev.* **2011**, *255*, 1713.
- (11) (a) Lescouëzec, R.; Toma, L. M.; Vaissermann, J.; Verdaguer, M.; Delgado, F. S.; Ruiz-Pérez, C.; Lloret, F.; Julve, M. *Coord. Chem. Rev.* **2005**, *249*, 2691. (b) Kim, J.; Han, S.; Pokhodnya, K. I.; Migliori, J. M.; Miller, J. S. *Inorg. Chem.* **2005**, *44*, 6983. (c) Jiang, L.; Choi, H. J.; Feng, X.-L.; Lu, T.-B.; Long, J. R. *Inorg. Chem.* **2007**, *46*, 2181. (d) Toma, L. M.; Lescouëzec, R.; Uriel, S.; Llusar, R.; Ruiz-Pérez, C.; Vaissermann, J.; Lloret, F.; Julve, M. *Dalton Trans.* **2007**, 3690. (e) Xiang, H.; Wang, S.-J.; Jiang, L.; Feng, X.-L.; Lu, T.-B. *Eur. J. Inorg. Chem.* **2009**, 2074.
- (12) (a) Wang, S.; Zuo, J.-L.; Zhou, H.-C.; Song, Y.; Gao, S.; You, X.-Z. *Eur. J. Inorg. Chem.* **2004**, *43*, 3681. (b) Wang, S.; Zuo, J.-L.; Zhou, H.-C.; Song, Y.; You, X.-Z. *Inorg. Chim. Acta* **2005**, *358*, 2101. (c) Ni, Z.-H.; Kou, H.-Z.; Zhao, Y.-H.; Zheng, L.; Wang, R.-J.; Cui, A.-L.; Sato, O. *Inorg. Chem.* **2005**, *44*, 2050. (d) Li, D.; Clérac, R.; Parkin, S.; Wang, G.; Yee, G. T.; Holmes, S. M. *Inorg. Chem.* **2006**, *45*, 5251. (e) Gu, J.-Z.; Jiang, L.; Tan, M.-Y.; Lu, T.-B. *J. Mol. Struct.* **2008**, *890*, 24. (f) Kang, L.-C.; Chen, X.; Wang, C.-F.; Zhou, X.-H.; Zuo, J.-L.; You, X.-Z. *Inorg. Chim. Acta* **2009**, *362*, 5195.
- (13) (a) Li, D.; Parkin, S.; Wang, G.; Yee, G. T.; Prosvirin, A. V.; Holmes, S. M. *Inorg. Chem.* **2005**, *44*, 4903. (b) Zhang, Y.-Z.; Malik, U. P.; Rath, N. P.; Clérac, R.; Holmes, S. M. *Inorg. Chem.* **2011**, *50*, 10537. (c) Pardo, E.; Verdaguer, M.; Herson, P.; Rousselière, H.; Cano, J.; Julve, M.; Lloret, F.; Lescouëzec, R. *Inorg. Chem.* **2011**, *50*, 6250.
- (14) (a) Li, D.; Parkin, S.; Wang, G.; Yee, G. T.; Clérac, R.; Wernsdorfer, W.; Holmes, S. M. *J. Am. Chem. Soc.* **2006**, *128*, 4214. (b) Zhang, Y.-Z.; Mallik, U. P.; Clérac, R.; Rath, N. P.; Holmes, S. M. *Chem. Commun.* **2011**, 47, 7194.
- (15) Yang, J. Y.; Shores, M. P.; Sokol, J. J.; Long, J. R. *Inorg. Chem.* **2003**, *42*, 1403.
- (16) (a) Wang, C.-F.; Gu, Z.-G.; Lu, X.-M.; Zuo, J.-L.; You, X.-Z. *Inorg. Chem.* **2008**, *47*, 7957. (b) Zhang, Y.; Mallik, U. P.; Rath, N.; Yee, G. T.; Clérac, R.; Holmes, S. M. *Chem. Commun.* **2010**, *46*, 4953. (c) Wu, D.; Zhang, Y.; Huang, W.; Sato, O. *Dalton Trans.* **2010**, *39*, 5500. (d) Costa, V.; Lescouëzec, R.; Vaissermann, J.; Herson, P.; Journaux, Y.; Araujo, M. H.; Clemente-Juan, J. M.; Lloret, R.; Julve, M. *Inorg. Chim. Acta* **2008**, *361*, 3912.
- (17) (a) Li, D.; Clérac, R.; Roubeau, O.; Harté, E.; Mathonière, C.; Le Bris, R.; Holmes, S. M. *J. Am. Chem. Soc.* **2008**, *130*, 252. (b) Zhang, Y.; Li, D.; Clérac, R.; Kalisz, M.; Mathonière, C.; Holmes, S. M. *Angew. Chem., Int. Ed.* **2010**, *49*, 3752. (c) Mercuriol, J.; Li, Y.; Pardo, E.; Risset, O.; Seuleiman, M.; Rousselière, H.; Lescouëzec, R.; Julve, M. *Chem. Commun.* **2010**, *46*, 8995. (d) Nihei, M.; Sekine, Y.; Suganami, N.; Nakazawa, K.; Nakao, H.; Murakami, Y.; Oshio, H. *J. Am. Chem. Soc.* **2011**, *133*, 3592.
- (18) Lescouëzec, R.; Vaissermann, J.; Toma, L. M.; Carrasco, R.; Lloret, F.; Julve, M. *Inorg. Chem.* **2004**, *43*, 2234.
- (19) Ni, Z.-H.; Kou, H.-Z.; Zhang, L.-F.; Ni, W.-W.; Jiang, Y.-B.; Cui, A.-L.; Ribas, J.; Sato, O. *Inorg. Chem.* **2005**, *44*, 9631.
- (20) Kim, J. I.; You, H. S.; Koh, E. K.; Kim, H. C.; Hong, C. S. *Inorg. Chem.* **2007**, *46*, 8481.
- (21) Kim, J. I.; You, H. S.; Koh, E. K.; Hong, C. S. *Inorg. Chem.* **2007**, *46*, 10461.
- (22) Kim, J. I.; Kwak, H. Y.; Yoon, J. H.; Ryu, D. W.; You, I. Y.; Yang, N.; Cho, B. K.; Park, J.-G.; Lee, H.; Hong, C. S. *Inorg. Chem.* **2009**, *48*, 2956.
- (23) Pichon, C.; Senapati, T.; Ababei, R.; Mathonière, C.; Clérac, R. *Inorg. Chem.* **2012**, *51*, 3796.
- (24) (a) Addison, A. W.; Burke, P. J. *J. Heterocyclic Chem.* **1981**, *18*, 803. (b) Panja, A.; Goswami, S.; Shaikh, N.; Roy, P.; Manassero, M.; Butcher, R. J.; Banerjee, P. *Polyhedron* **2005**, *24*, 2912.
- (25) Otwinowski, Z.; Minor, W. *Methods in Enzymology*; Carter, C. W., Jr., Sweet, R. M., Eds.; Academic Press: New York, 1997; Vol. 276, pp 307–326.
- (26) Sheldrick, G. M. *SHELXL97, Program for Crystal Structure Refinement*; University of Göttingen: Göttingen, Germany, 1997.
- (27) Farrugia, L. J. *J. Appl. Crystallogr.* **1999**, *32*, 837.
- (28) (a) Gu, Z.-G.; Liu, W.; Yang, Q.-F.; Zhou, X.-H.; Zuo, J.-L.; You, X.-Z. *Inorg. Chem.* **2007**, *46*, 3236. (b) Wang, C.-F.; Liu, W.; Song, Y.; Zhou, X.-H.; Zuo, J.-L.; You, X.-Z. *Eur. J. Inorg. Chem.* **2008**, 717.
- (29) Wang, X.; Wang, S.; Li, L.; Sundberg, E. B.; Gacho, G. P. *Inorg. Chem.* **2003**, *42*, 7799.
- (30) (a) Lu, T.; Xiang, H.; Su, C.; Cheng, P.; Mao, Z.; Ji, L. *New J. Chem.* **2001**, 216. (b) Ohba, M.; Iwamoto, T.; Okawa, H. *Chem. Lett.* **2002**, *10*, 1046. (c) Berlinguette, C. P.; Galán-Mascarós, J. R.; Dunbar, K. R. *Inorg. Chem.* **2003**, *42*, 3416. (d) Li, D.; Parkin, S.; Clérac, R.; Holmes, S. M. *Inorg. Chem.* **2006**, *45*, 7569.
- (31) (a) Colacio, E.; Domínguez-Vera, J. M.; Lloret, F.; Rodríguez, A.; Stoeckli-Evans, H. *Inorg. Chem.* **2003**, *42*, 6962. (b) Liu, W.; Wang, C.-F.; Li, Y.-Z.; Zuo, J.-L.; You, X.-Z. *Inorg. Chem.* **2006**, *45*, 10058. (c) Li, D.; Clérac, R.; Wang, G.; Yee, G. T.; Holmes, S. M. *Eur. J. Inorg. Chem.* **2007**, 1341. (d) Hoshino, N.; Sekine, Y.; Nihei, M.; Oshio, H. *Chem. Commun.* **2010**, *46*, 6117.
- (32) (a) Bartlett, B. M.; Harris, T. D.; De Groot, M. W.; Long, J. R. *Z. Anorg. Allg. Chem.* **2007**, *633*, 2380. (b) Kim, J.; Han, S.; Lim, J. M.; Choi, K.-Y.; Nojiri, H.; Suh, B. J. *Inorg. Chim. Acta* **2007**, *360*, 2647.
- (33) (a) Kou, H. -Z.; Gao, S.; Ma, B.-Q.; Liao, D.-Z. *Chem. Commun.* **2000**, 1039. (b) Toma, L. M.; Lescouëzec, R.; Armentano, D.; De Munno, G.; Andruh, M.; Cano, J.; Lloret, F.; Julve, M. *Dalton Trans.* **2005**, 1357.
- (34) (a) Koo, J.; Kim, D.; Kim, Y.-S.; Do, Y. *Inorg. Chem.* **2003**, *42*, 2983. (b) Saha, M. K.; Morón, M. C.; Palacio, F.; Bernal, I. *Inorg. Chem.* **2005**, *44*, 1354.
- (35) Kahn, O. *Molecular Magnetism*; VCH Publishers: New York, 1993; pp 211–213.
- (36) (a) Rodríguez-Diéguez, A.; Kivekäs, R.; Sillanpää, R.; Cano, J.; Lloret, F.; McKee, V.; Stoeckli-Evans, H.; Colacio, E. *Inorg. Chem.* **2006**, *45*, 10537. (b) Atanasov, M.; Busche, C.; Comba, P.; Hallak, F. E.; Martin, B.; Rajaraman, G.; van Slageren, J.; Wadepohl, H. *Inorg. Chem.* **2008**, *47*, 8112.
- (37) Borrás-Almenar, J. J.; Clemente-Juan, J. M.; Coronado, E.; Tsukerblat, B. S. *J. Comput. Chem.* **2001**, *22*, 985.
- (38) Peng, Y.-H.; Meng, Y.-F.; Hu, L.; Li, Q.-X.; Li, Y.-Z.; Zuo, J.-L.; You, X.-Z. *Inorg. Chem.* **2010**, *49*, 1905.
- (39) Rogez, G.; Rebillay, J.-N.; Barra, A.-L.; Sorace, L.; Blondin, G.; Kirchner, N.; Duran, M.; van Slageren, J.; Parsons, S.; Ricard, L.; Marvilliers, A.; Mallah, T. *Angew. Chem., Int. Ed.* **2005**, *45*, 1876.
- (40) Seiden, J. J. *Phys. (Paris)* **1983**, *44*, L 947.
- (41) Jeannin, O.; Clérac, R.; Cauchy, T.; Fourmigué, M. *Inorg. Chem.* **2008**, *47*, 10656.